Diagnosis of laser-compressed shells based on absorption of core radiation

B. Yaakobi, R. Epstein, and F. J. Marshall
Laboratory for Laser Energetics, University of Rochester, 250 East River Road, Rochester, New York 14623
(Received 2 July 1991)

A diagnostic method for laser-imploded targets, particularly plastic shells, is described. It is based on the observation of a peak in the continuum x-ray spectrum emitted from the target. The peak is the result of the high absorption of low-energy x rays from the implosion core by the cooler, compressed shell surrounding the core. In glass targets, where the shell absorption is typically dominated by bound-free transitions (photoionization), the position of this peak in the spectrum depends on the shell $\rho\Delta r$. In plastic targets, where the shell absorption is due mainly to free-free transitions (inverse bremsstrahlung), the position of the peak depends on the $\rho^2\Delta r/T^{1/2}$ for the shell. We study the relationship between the position of the peak and these two quantities, both analytically as well as with a simulation code.

PACS number(s): 52.50.Jm

A method for diagnosing laser-driven target implosions, particularly of plastic shells, is described. It is based on the fact that most x-ray emission from the core is absorbed by the dense, cooler compressed shell surrounding the core. The core radiation is emitted by the fuel and (mainly) by the inner layer of the compressed shell, and is absorbed by the rest of the compressed shell which is at a lower temperature. Since the shell is transparent to harder radiation, a peak should be observed in the emerging x-ray spectrum [1]. This peak would shift to higher photon energy, as the achieved compression becomes greater. The method is particularly useful for plastic targets $(CH)_n$ on which we concentrate in this work. This is because in glass shells, as shown below, the inferred cold-shell $\rho\Delta r$ can be much smaller than the total shell $\rho\Delta r$, reducing the usefulness of the method. Also, fuel-filled plastic targets do not provide line emission diagnostics, so alternative methods such as this are desirable. It might be thought that the measurement in the case of glass shells is easier because of the much higher emission than from CH targets at the same wavelength. However, the absorption is also much greater in glass, and the position of the peak is reached at higher photon energies, where core emission becomes weaker.

The absorption of x rays in the shell is due to either photoionization (bound-free transitions) in partially ionized material or inverse bremsstrahlung (free-free transitions) due to the free electrons. In glass-shell targets, the atoms in the cold part of the imploded shell are typically not completely stripped. Therefore, the absorption is predominantly due to K-shell photoionization, for which the opacity is proportional to the density ($k_{bf}\sim\rho$). In plastic targets, the absorbing shell can be sufficiently hot for the carbon atoms to be highly ionized. For completely stripped ions, the dominant x-ray-absorption mechanism is inverse bremsstrahlung, for which the opacity depends on both density and temperature ($k_{ff}\sim\rho^2/T^{1/2}$). The location of the spectral peak is shown below to occur at a wavelength where the optical depth is about 1. Thus, the location of the peak in the emission from glass shells should depend on the shell $\rho\Delta r$ (or more precisely, the integral $\int\rho\,dr$) of the cold part of the imploded glass shell. In highly ionized plastic shell material, the position of the peak would be a function of the quantity $\rho^2\Delta r/T^{1/2}$ for the shell. Because of the weak dependence on T, it would effectively be a function of the $\rho^2\Delta r$ (or more precisely, the integral $\int\rho^2 dr$) of the imploded shell.

Since the method relates only to the cold, absorbing part of the shell, we address the question of what fraction of the shell is absorbing. In the case of CH shells, because of the weak dependence of inverse bremsstrahlung absorption on temperature, the hotter, inner layer of the imploded shell can contribute significantly to the total absorption. The cold-shell $\rho^2\Delta r$ value obtained from the position of the peak will thus not be much smaller than that of the total CH shell. On the other hand, the inner, hot layer of an imploded glass shell will have negligible photoionization absorption (because of its atoms being stripped); thus, the $\rho\Delta r$ value derived from the peak will be considerably smaller than that of the total glass shell. This is an additional advantage in applying this method to CH as compared with glass shells.

In general, the importance of inverse bremsstrahlung with respect to photoionization increases with temperature, since the increased ionization reduces the density of ions which can undergo photoionization. In competition with this, the actual opacity due to inverse bremsstrahlung at fixed ionization actually decreases with an increase in the temperature. Inverse bremsstrahlung also becomes more important with an increase in density, for a fixed ionization, because of the different dependences on ρ. However, for a given temperature, the ionization [in local thermodynamic equilibrium (LTE)] decreases with an increase in the density; this tends to increase the relative importance of photoionization absorption.

The opacity due to inverse bremsstrahlung (free-free transitions) is given by [2]

$$k_{ff}=(4\pi Z^2e^6g/3^{3/2}hcm^2\nu^3)(2m/\pi kT)^{1/2}N_eN_i\ , \qquad (1)$$

where g is a Gaunt factor [3] and where the other symbols have their usual meaning. For photon energies much higher than kT (as is the case in the absorbing shell), g is very nearly equal to 1, and Eq. (1) can be written

$$k_{ff}(\mathrm{cm}^{-1})=4.02\times10^{-51}Z^2N_eN_i\lambda^3/T^{1/2}\ , \qquad (2)$$

where λ is in Å, N_e and N_i are in cm^{-3}, and T is in keV. For a multispecies target, $Z^2N_eN_i$ is replaced by $N_e^2\langle Z^2\rangle_{\mathrm{av}}/\langle Z\rangle_{\mathrm{av}}$ in terms of species averages. For a CH target, in terms of the mass density ρ ($\mathrm{g\,cm}^{-3}$), we find (assuming fully ionized CH)

$$k_{ff}(\mathrm{cm}^{-1})=A_{\mathrm{CH}}\lambda^3\rho^2/T^{1/2}\ , \tag{3}$$

where $A_{\mathrm{CH}}=2.23\times10^{-3}$. From Eq. (3), an optical depth $\tau=k\Delta r$ of 1 will occur in CH at the photon energy E_1 (keV) given by

$$\rho^2\Delta r/T^{1/2}=0.24E_1^3\ . \tag{4}$$

Because of the assumption of full ionization, Eq. (4) would be valid for temperatures higher than $\sim$200 eV. As an example, assume an imploded CH shell target with $T=0.3$ keV, $\rho\Delta r=0.05$ $\mathrm{g\,cm}^{-2}$, and $\rho=50$ $\mathrm{g\,cm}^{-3}$; E_1 would then be at 2.66 keV.

The proposed diagnostic method relates the observed photon energy of the peak $E_{\max}$, to E_1, from which the quantity $\rho^2\Delta r/T^{1/2}$ for the shell is derived. Obviously, the optical depth at the peak would be of order 1: for photon energies lower than $E_{\max}$ the intensity falls because the optical depth is higher than 1, whereas above $E_{\max}$ the falling continuum is just the unattenuated core-emission spectrum. Because of the weak dependence on T, a crude knowledge of the temperature yields the quantity $\rho^2\Delta r$ through the cold part of the shell. This quantity, in conjunction with a separate determination of the $\rho\Delta r$ (for example, from nuclear activation) can be used to estimate the shell density. However, it should be noted that the nuclear activation technique measures $\rho\Delta r$ of the entire shell, not only its cold part.

In imploded glass shells with $T\sim300$ eV (in the outer part of the imploded shell), silicon atoms will not be fully ionized (i.e., a significant fraction will have at least one bound electron), and photoionization will dominate the absorption. The photoionization opacity for energies above the Si K edge is then approximately given by the opacity of cold glass [4] multiplied by a correction factor α. This factor is given in terms of the opacity due to the K and L shells, $\alpha=k_K/k_{K+L}$. From the measured opacity jump of cold material at the K edge, we find $\alpha=0.91$, and thus (from Ref. [4]) $k_{bf}=8.76\lambda^3\rho$ (λ in Å). This equation applies to glass with mostly heliumlike silicon ions. If most of the silicon ions are hydrogenlike, the opacity will be one-half of this; however, in typical cases the cold part of the imploded glass shell has only a small percentage of hydrogenlike silicon ions and the hotter layers which do have, contribute little to the overall opacity. An optical depth of 1 will be attained at an energy E_1 given by

$$E_1(\mathrm{keV})=25.5(\rho\Delta r)^{1/3}\ . \tag{5}$$

Because of the assumption of little ionization of K-shell silicon ions, Eq. (5) would be valid for temperatures lower than $\sim$500 eV. For $\rho\Delta r=0.05$ $\mathrm{g\,cm}^{-2}$ this relation gives $E_1=9.4$ keV, much higher than E_1 for the plastic shell example given above. At this high photon energy, the emitted intensity is small and difficult to detect above the background; this background is due mostly to radiation from the laser-target interaction region, and is higher for glass targets. Time-resolved spectroscopy can be used to greatly reduce the background problem.

In order to relate E_1 to $E_{\max}$, the photon energy of the spectral peak, we approximate the emitted spectrum by the relation

$$I=I_0\exp(-E/T_c)\exp[-(E_1/E)^3]\ . \tag{6}$$

The first factor approximates the unattenuated x-ray flux as that emitted by a hot plasma at a single core temperature T_c (which is higher than the temperature T of the absorbing shell); the second factor accounts for the shell absorption and follows from Eq. (1) and the definition of E_1. It should be emphasized that, for typical fuel-filled CH shells, most of the core radiation is emitted by the inner CH layer and thus T_c is lower than the peak fuel temperature. However, in very high-density compressions the fuel emission can dominate the emission from the core, and T_c will then correspond to the fuel temperature. The emergent spectrum I of Eq. (6) has a peak, $E_{\max}$, given by

$$(E_{\max}/E_1)=(3T_c/E_1)^{1/4}\ . \tag{7}$$

To relate the measured $E_{\max}$ to E_1, T_c can be determined from the continuum slope at photon energies above the peak, and Eq. (7) can then be solved for E_1. The $(E_{\max}/E_1)$ ratio is typically close to 1 (see below).

The assumption of negligible photoionization opacity in CH shells deserves some scrutiny. Since the cross section for photoionization is typically much larger than that for inverse bremsstrahlung, the former will be negligible only if the plastic shell is highly ionized everywhere. An ionization rate equation code (POPION [5]) has shown that the ionization of carbon at the expected temperatures of the compressed plastic shell is incomplete. For example, at a temperature of 200 eV and an electron density of $1\times10^{24}\,\mathrm{cm}^{-3}$, the fraction of carbon ions in the hydrogenlike state is 32% and at 300 eV it is 14% (most of the rest is stripped). We now estimate the ratio of the two opacity contributions, k_{bf} due to photoionization, and k_{ff} due to inverse bremsstrahlung. k_{ff} is given by Eq. (3) where ρ is now written as ρ_s, the density of completely ionized (stripped) material. k_{bf} is taken as the measured opacity [4] of cold CH, in terms of the density ρ_{us} of the unstripped carbon, multiplied by the correction factor $\alpha=0.96$, then divided by 2 (because most of the unstripped carbon will be in the hydrogenlike state, whereas the cold material formula assumes two K-shell electrons):

$$k_{bf}=0.54\lambda^3\rho_{us}\ , \tag{8}$$

so that the ratio of the two becomes

$$R_k=k_{bf}/k_{ff}=242(T^{1/2}/\rho_s)(\rho_{us}/\rho_s)\ . \tag{9}$$

As an example, assuming $T=0.2$ keV and a fraction of unstripped material of 0.2, R_k will be smaller than 1 only at densities higher than 22 $\mathrm{g\,cm}^{-3}$. Thus, a more detailed calculation with a numerical code is required to determine the relative importance of these two absorption mechanisms for target experiments of lower densities.

We next compare the location of the peak as predicted by Eqs. (4) or (5) with that predicted by a hydrodynamic

code (LILAC), run in conjunction with a non-LTE post processor which calculates the emergent radiation spectrum [6]. We first simulate the implosion of a DD-filled CH shell. Figure 1 shows the calculated, time-integrated emergent spectrum from a CH shell of 10-μm thickness and 250-μm diameter, filled with 40-atm pressure of D_2, irradiated by a 1.25-kJ, 625-ps (FWHM) laser pulse ($\lambda=351$ nm). As the results show, a peak indeed appears in the emitted spectrum. It should be noted that the computed spectrum results from radiation transport treatment which sums over rays of different impact parameters (the ray geometry can be described as a set of concentric cylinders intersecting the spherical target). Thus, it corresponds to a spectral measurement without any spatial resolution. Obviously, even with no such resolution, a peak in the spectrum should be evident. However, spatial resolution would increase the contrast of the peak in the spectrum, the most distinct peak being in the spectrum viewed through the target center. The two additional curves in Fig. 1 correspond to simulations where the contribution of only free-free or only bound-free transitions to the opacity were included. It is clear that the contribution of free-free transitions accounts for much of the opacity. By removing either contribution to the opacity, the emergent radiation suffers less attenuation in the shell and is therefore stronger; also, the peak shifts to lower photon energies, where the absorption is higher. The peak E_1 given by Eq. (4) can now be compared with the peak of the curve marked FF in Fig. 1. The integral $\int \rho^2 dr$ over the entire CH shell of Fig. 1, at peak compression, was calculated by the code to be 1.27 $g^2\,cm^{-5}$. Substituting into Eq. (4), and using the average simulated shell temperature at peak compression of 0.35 keV, we obtain $E_1=2.08$ keV. The continuum slope in Fig. 1 gives $T_c=1.2$ keV, and Eq. (7) then yields $E_{max}=2.38$. This position of the peak agrees to within better than 10% with the peak in the simulated spectrum marked FF in Fig. 1. This agreement indicates that the time-integrated spectrum can be used to derive the $\rho^2\Delta r$ value at the time of peak compression. In fact, a closer examination of the computation shows that the peak is typically formed over a $\sim$50-ps period around peak compression; time integration reduces the ratio of peak height to background but has little effect on the position of the peak. This agreement also shows that the derived $\rho^2\Delta r$ value (which is only related to the absorbing part of the shell), is only slightly less than that for the total shell thickness. Indeed, the computations show that, around peak compression, the inner third of the shell is hot ($\sim$1 keV) and is the source of the emitted continuum. As discussed above, even the hot CH layer contributes to the continuum absorption, so the derived value of $\rho^2\Delta r$ (relating only to the absorbing layer) is quite close to the $\rho^2\Delta r$ for the entire shell thickness.

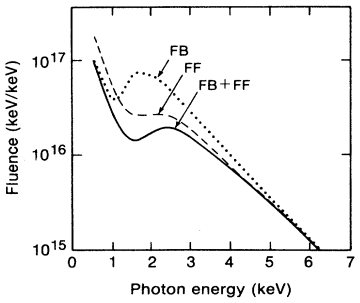

FIG. 1. Calculated emergent spectrum (time integrated) from a CH shell of 10-μm thickness and 250-μm diameter, filled with 40-atm pressure of D_2, irradiated by a 1.25-kJ, 625-ps laser ($\lambda=351$ nm). For the curve marked FB, only the bound-free contribution to the opacity was included in the simulation; for the curve marked FF, only the free-free contribution to the opacity was included. The curve marked FB+FF corresponds to the full calculation.

We next verify that, as expected, the peak in the emergent spectrum shifts to higher photon energies for higher compression implosions. To that end, we compare in Fig. 2 the spectrum from Fig. 1 with that of a thicker CH shell, imploded by a higher-energy laser: the shell thickness is now 15 μm (as compared with 10 μm), and the laser energy is now 1.87 kJ, as compared with 1.25 kJ. All other parameters are the same for the two simulations. Note that unlike Fig. 1, the results of Fig. 2 are not time integrated, but show the spectral energy per ns at the time of peak compression. The integral $\int \rho^2 dr$ over the thicker CH shell, at peak compression, was calculated by the simulation to be 5.95 $g^2\,cm^{-5}$ (as compared with 1.27 $g^2\,cm^{-5}$ for the thinner shell above). The temperature is also higher, 0.64 keV as compared with 0.34 keV. Using Eqs. (4) and (7) as before, we find $E_{max}=3.25$ keV, in good agreement with the thicker-shell curve of Fig. 2. Comparison of Figs. 1 and 2 shows that, even though the peak is still visible in the time-integrated results, a better contrast would be obtained with a time-resolved measurement; however, the position of the peak itself is hardly affected.

Finally, we simulate the implosion of a CH-coated glass shell, where the glass absorption of the core radiation is mostly due to photoionization. Figure 3 shows the time-integrated emergent x-ray spectrum. The target parameters were a glass shell of 1.79-μm thickness and 244-μm diameter, overcoated with a 6-μm-thick CH layer and a 0.05-μm-thick layer of aluminum, and filled with 80-atm pressure of DT. The target was irradiated by a 1.66-kJ, 625-ps (FWHM) laser pulse at $\lambda=351$ nm. Fig-

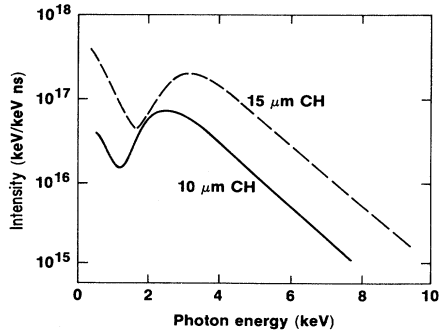

FIG. 2. Comparison of the calculated emergent spectrum (per ns at the time of peak compression) from the shell of Fig. 1, and from a 15-μm-thick shell irradiated with a 1.87-kJ laser pulse. All other parameters are the same for the two shots.

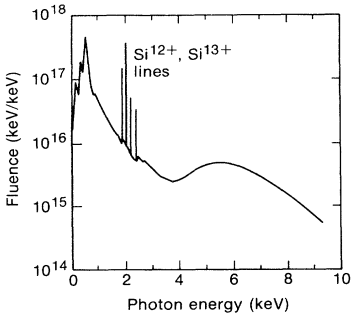

FIG. 3. Calculated emergent spectrum (time integrated) from a glass shell of 1.79-μm thickness and 244-μm diameter, overcoated with a 6-μm thick CH layer and a 0.05-μm thick layer of aluminum, filled with 40-atm pressure of D_2. The target was irradiated by a 1.66-kJ, 625-ps laser ($\lambda = 351$ nm).

ure 3 shows a peak due to the shell absorption, at an energy of 5.5 keV. The slope of the continuum above 6 keV corresponds to a core temperature of 1.4 keV. Using Eq. (7) we find $E_1 = 6.0$ keV. From Eq. (5) we derive $\rho\,\Delta r = 13$ mg/cm^2 for the cold part of the glass shell (i.e., the part of the shell where higher ionizations than the heliumlike state are negligible). The LILAC simulation for this target implosion yields $\rho\,\Delta r$ of 54 mg/cm^2 at peak compression, considerably higher than the inferred $\rho\,\Delta r$. A closer examination of the calculated temperature profiles can account for this discrepancy. The temperature of most of the glass shell is ~ 1 keV and drops to ~ 0.2 keV near the glass-CH interface. At the time of peak compression, only the outer layer (about one-third) of the glass shell can contribute to photoionization, i.e., has appreciable population of ground-state heliumlike silicon ions. In the remainder of the glass shell, much of the heliumlike and hydrogenlike ions are excited and contribute little to bound-free absorption (the cross section of which depends on the principal quantum number as n^{-5}). In view of the appreciable ionization in the glass, we need to reexamine the assumption that the observed absorption in glass is due primarily to photoionization rather than to inverse bremsstrahlung. Equation (3) rederived for glass gives $A_{\text{glass}} = 3.93$, and with an average glass temperature of 0.6 keV, we now find $\rho^2\,\Delta r = 22\ \text{g}^2\,\text{cm}^{-5}$, as compared with the LILAC value at peak compression of only $2.36\ \text{g}^2\,\text{cm}^{-5}$. This discrepancy shows that, for this simulated glass-shell implosion, photoionization is indeed the dominant mechanism even with significant ionization because, with inverse bremsstrahlung alone, we would infer too high a value of $\rho^2\,\Delta r$ as compared with the code determination. Because the contribution from the hot part of the glass shell to photoionization absorption is negligible (and its absorption by inverse bremsstrahlung is even smaller), the $\rho^2\,\Delta r$ derived from the peak is substantially smaller than the total shell $\rho^2\,\Delta r$.

The comparison with the code simulations shows, thus, that the simple relationship for CH shells given by Eq. (4) provides a fairly good estimate of the shell $\rho^2\,\Delta r$. However, in the case of glass targets, the position of the peak from Eq. (5) may significantly underestimate the shell $\rho\,\Delta r$. In actual application of the method, the measured position of the peak will be compared with the results of full simulations. In the case of agreement in the position of the peak, we can surmise (especially in the case of CH shells) that the predicted $\rho\,\Delta r$ (or $\rho^2\,\Delta r$) has been achieved. However, in the case where the two disagree (because of a degradation in implosion performance), Eq. (4) could be used to estimate the reduction in $\rho^2\,\Delta r$ [or Eq. (5), the reduction in $\rho\,\Delta r$], corresponding to a measured shift in $E_{\max}$ with respect to the predicted value.

The applicability of the method for cases of instability and shell-fuel mixing requires special attention. If the instability does not lead to shell breakup or severe shell distortion, and a peak in the emitted spectrum is still observed, it is very likely that Eq. (4) will still be applicable. The instability in this case will be manifest by a reduced shell $\rho^2\,\Delta r$ (or $\rho\,\Delta r$) and a reduced core temperature (due to either radiation cooling or incomplete conversion of kinetic to thermal energy). The position of the peak will then show the reduced $\rho^2\,\Delta r$ (by appearing at a lower photon energy) and the continuum slope beyond the peak will show the reduced core temperature. The application of Eq. (4) is valid provided that the carbon in the target is almost completely stripped. This requires the temperature in the cold part of the CH shell to exceed ~ 200 eV. The application of Eq. (5) to determine the $\rho\,\Delta r$ of the cold part of the shell only requires that silicon ions there have at least two bound electrons, or that the temperature be lower than ~ 500 eV. Thus, the achievement of lower than predicted temperature because of instability will only improve the applicability of Eq. (5), and will invalidate Eq. (4) only if the cooling were very severe.

Severe shell deformation could be demonstrated by observing a different position of the peak in the spectrum when viewed from two different directions. Shell breakup will result in smearing and eventually the disappearance of the spectral peak. This is because different parts of the core radiation now traverse different $\rho\,\Delta r$ segments, leading to peaks of different spectral position. Thus, an indistinct peak in the observed spectrum could be indicative of an unstable implosion.

This work was supported by the U.S. Department of Energy Division of Inertial Fusion under Agreement No. DE-FC03-85DP40200 and by the Laser Fusion Feasibility Project at the Laboratory for Laser Energetics which has the following sponsors: Empire State Electric Energy Research Corporation, New York State Energy Research and Development Authority, Ontario Hydro, and the University of Rochester.

[1] Laboratory for Laser Energetics LLE Review 24, Quarterly Report No. DOE/DP40200-04, 1985 (unpublished), pp. 169–179.

[2] L. Spitzer, *Physics of Fully Ionized Gases,* 2nd ed. (Interscience, New York, 1962), p. 148.

[3] W. J. Karzas and R. Latter, Astrophys. J. Supp. **6**, 167 (1961).

[4] B. L. Henke and R. L. Elgin, Adv. X-Ray Anal. **13**, 1 (1969).

[5] R. Epstein, S. Skupsky, and J. Delettrez, J. Quant. Spectrosc. Radiat. Transfer **35**, 131 (1986).

[6] R. Epstein, Phys. Fluids B **1**, 214 (1989).